Inorg. Chem. **2003**, *42*, 6123–6129

Coexistence of Long-Range Ferromagnetic Ordering and Glassy Behavior in One-Dimensional Bimetallic Cyano-Bridged Polymers

Dongfeng Li,*,† Limin Zheng,† Yuanzhu Zhang,‡ Jin Huang,† Song Gao,*,‡ and Wenxia Tang†,§

State Key Laboratory of Coordination Chemistry, Nanjing University, Nanjing 210093, People's Republic of China, and State Key Laboratory of Rare Earth Materials Chemistry and Applications, College of Chemistry and Molecular Engineering, Peking University, Beijing 100871, People's Republic of China

Received May 19, 2003

Two new one-dimensional (1-D) 3d–5d cyano-bridged bimetallic assemblies, $\{[Co_3^{II}(DMF)_{12}][W^V(CN)_8]_2]\}_\infty$ (**1**) and $\{[Mn_3^{II}(bipy)_2(DMF)_8][W^V(CN)_8]_2\}_\infty$ (**2**), have been synthesized and characterized, where bipy stands for 2,2′-bipyridine and DMF represents *N*,*N*-dimethylformamide. The X-ray analyses show that the two complexes belong to the $P\bar{1}$ space group with $Z = 1$ and $C_{52}H_{84}N_{28}O_{12}Co_3W_2$, $a = 11.690(3)$ Å, $b = 12.703(3)$ Å, $c = 13.712(3)$ Å, $\alpha = 86.889(4)°$, $\beta = 73.256(4)°$, and $\gamma = 77.033(4)°$ for **1** and $C_{60}H_{72}N_{28}O_8Mn_3W_2$, $a = 10.672(2)$ Å, $b = 13.024(3)$ Å, $c = 16.000(3)$ Å, $\alpha = 78.32(3)°$, $\beta = 75.69(3)°$, and $\gamma = 66.63(3)°$ for **2**. The structures of the two complexes are similar and consist of 12-atom rhombic $M_2W_2(CN)_4$ (M = Co (**1**), Mn (**2**)) units, which act as a basic component to be repeatedly connected through W–C–N–M–N–C–W linkages to form a one-dimensional infinite 3,2-chain; these chains are well separated by the DMF molecules or 2,2′-bipyridines coordinated to the metal ions Co^{2+} for **1** and Mn^{2+} for **2**. Magnetic studies, including linear and nonlinear ac susceptibility measurements, demonstrate that the long-range magnetic ordering and spin glass behavior coexist in the two 1-D compounds.

Introduction

The design and elaboration of new molecule-based magnetic materials has been an active area of research from both a fundamental and potential application perspective during the past decade. Over the past few years, hexacyanometalates ($[M(CN_6)]^{n-}$, M = Fe, Mn, Co, etc.), acting as good building blocks, have been used to construct a family of molecule-based magnets with interesting structures and properties,[1,2] such as the discovery of the magnetic−optical phenomenon,[1f] the finding of a molecule-based magnet with bulk magnetism at T_C over 100 °C,[1i] and single-molecule magnet behavior at low temperature.[1k] Recently, the magnetism of 3d−4d/5d bimetallic cyano-bridged assemblies derived from octacyanometalates ($[M(CN)_8]^{n-}$, M = Mo, W) has attracted much attention, due to the d orbital of their central 4d/5d metal ions being more diffuse than that of 3d metal ions[3] and their versatility in geometry,[4] as well as their photoresponsive

* To whom correspondence should be addressed. E-mail: chem1121@nju.edu.cn (D.L.); gaosong@pku.edu.cn (S.G.). Fax: +86-25-331-4502.
† Nanjing University.
‡ Peking University.
§ Deceased.

(1) For example: (a) Gadet, V.; Mallah, T.; Castro, I.; Verdaguer, M. *J. Am. Chem. Soc.* **1992**, *114*, 9213. (b) Mallah, T.; Thiébaut, S.; Verdaguer, M.; Veillet, P. *Science* **1993**, *262*, 1554. (c) Ferlay, S.; Mallah, T.; Quahes, R.; Veillet, P.; Verdaguer, M. *Nature (London)* **1995**, *378*, 701. (d) Entley, W. R.; Girolami, G. S. *Science* **1995**, *268*, 397. (e) Verdaguer, M. *Science* **1996**, *272*, 698. (f) Sato, O.; Iyoda, T.; Fujishima, A.; Hashimoto, K. *Science* **1996**, *271*, 49. (g) Sato, O.; Iyoda, T.; Fujishima, A.; Hashimoto, K. *Science* **1996**, *272*, 704. (h) Dujardin, E.; Ferlay, S.; Phan, X.; Desplanches, C.; Cartier dit Moulin, C.; Sainctavit, P.; Baudelet, E.; Veillet, P.; Verdaguer, M. *J. Am. Chem. Soc.* **1998**, *120*, 11347. (i) Holmes, S. M.; Girolami, G. S. *J. Am. Chem. Soc.* **1999**, *121*, 5593.

(2) For example: (a) Ohba, M.; Maruono, N.; Ōkawa, H.; Enoki, T.; Latour, J.-M. *J. Am. Chem. Soc.* **1994**, *116*, 11566. (b) Miyasaka, H.; Matsumoto, N.; Ōkawa, H.; Re, N.; Gallo, E.; Floriani, C. *Angew. Chem., Int. Ed. Engl.* **1995**, *34*, 1446. (c) Miyasaka, H.; Matsumoto, N.; Ōkawa, H.; Re, N.; Gallo, E.; Floriani, C. *J. Am. Chem. Soc.* **1996**, *118*, 981. (d) Re, N.; Gallo, E.; Floriani, C.; Miyasaka, H.; Matsumoto, N. *Inorg. Chem.* **1996**, *35*, 5964. (e) Ohba, M.; Ōkawa, H.; Fukita, N.; Hashimoto, Y. *J. Am. Chem. Soc.* **1997**, *119*, 1011. (f) Ohba, M.; Usuki, N.; Fukita, N.; Ōkawa, H. *Angew. Chem., Int. Ed.* **1999**, *38*, 1795. (g) Zhang, S.-W.; Fu, D.-G.; Sun, W.-Y.; Hu, Z.; Yu, K.-B.; Tang, W.-X. *Inorg. Chem.* **2000**, *39*, 1142. (h) Inoue, K.; Imai, H.; Ghalsasi, P. S.; Kikuchi, K.; Ohba, M.; Ōkawa, H.; Yakhmi, J. V. *Angew. Chem., Int. Ed.* **2001**, *40*, 4242. (i) Kou, H.-Z.; Gao, S.; Zhang, J.; Wei, G.-H.; Su, G.; Zheng, R. K.; Zhang, X. X. *J. Am. Chem. Soc.* **2001**, *123*, 11809. (j) Thétiot, F.; Triki, S.; Sala Pala, J.; Gómez-García, C. J.; Golhen, S. *Chem. Commun.* **2002**, 1078. (k) Berlinguette, C. P.; Vaughn, D.; Cañada-Vilalta, C.; Gãlan-Mascarós, J. R.; Dunbar, K. R. *Angew. Chem., Int. Ed.* **2003**, *42*, 1523.

(3) Yeung, W.-F.; Man, W.-L.; Wong, W.-T.; Lau, T.-C.; Gao. S. *Angew. Chem., Int. Ed.* **2001**, *40*, 3031.

(4) Leipoldt, J. G.; Basson, S. S.; Roodt, A. *Adv. Inorg. Chem.* **1993**, *32*, 241.

10.1021/ic034539k CCC: $25.00
Published on Web 08/23/2003

properties.[5] Until now, compounds with various structures ranging from discrete entities to three-dimensional extended networks have been well documented, some of which exhibit intriguing magnetic properties, such as long-range magnetic ordering and ground spin state as high as $S = {}^{51}/_{2}$.[5−9]

In this report we present the new cyano-bridged 1-D $Co^{II}-W^{V}$ complex $\{[Co_3^{II}(DMF)_{12}][W^{V}(CN)_8]_2]\}_\infty$ (**1**; DMF = *N*,*N*-dimethylformamide). The magnetic study shows that compound **1** is frequency-dependent and exhibits magnetic hysteresis at low temperature, just like the "single-chain magnet" (SCM) behavior predicted in 1963 by Glauber and observed in 1-D Ising chain compounds reported recently by Clérac et al.[10] However, further measurements demonstrate that compound **1** is a ferromagnet with the coexistence of long-range ferromagnetic ordering and glassy behavior. Here, we report the syntheses, structures, and magnetic properties of complex **1** and its 1-D analogue $\{[Mn_3^{II}(bipy)_2(DMF)_8][W^{V}(CN)_8]_2\}_\infty$ (**2**; bipy = 2,2′-bipyridine).

Experimental Section

Materials and Instrumentation. The precursor $(n\text{-}Bu_4N)_3[W(CN)_8]$ was prepared according to published procedures.[11] Other starting materials were of analytical grade and were used without further purification. C, H, N elemental analyses were carried out with a Perkin-Elmer 240C elemental analyzer, and the contents of metal ions were analyzed on a HOBIN YVON JY38S ICP spectrometer. Infrared spectroscopy on KBr pellets was performed on a Bruker Vector 22 FT-IR spectrophotometer in the region 4000−400 cm^{-1}. The magnetic susceptibilities, ac magnetic susceptibility, and field dependence of magnetization up to 7 T at 1.8 K were obtained on crystalline samples using a Model MagLab System 2000 magnetometer. The experimental susceptibilities were corrected for the sample holder and the diamagnetism contributions estimated from Pascal's constants. Effective magnetic moments were calculated using the equation $\mu_{eff} = 2.828(\chi_M T)^{1/2}$, where χ_M is the molar magnetic susceptibility.

Preparation of $\{[Co_3(DMF)_{12}][W(CN)_8]_2$ (1). All of the following procedures were carried out in the dark to avoid decomposition of $(n\text{-}Bu_4N)_3[W(CN)_8]$. A solution of $Co(ClO_4)_2\cdot 6H_2O$ (55 mg, 0.15 mmol) in CH_3OH (2 mL) was added to a solution of $(n\text{-}Bu_4N)_3[W(CN)_8]$ (112 mg, 0.10 mmol) in CH_3OH (3 mL) under an inert atmosphere with stirring to give red polycrystalline material after several minutes, which was filtered and washed with methanol. Then the red product was dissolved in DMF. Well-shaped red block crystals were obtained by slow diffusion of diethyl ether into the resulting DMF solution for several days (yield 75%). Anal. Calcd for $C_{52}H_{84}N_{28}O_{12}Co_3W_2$: C, 33.98; H, 4.57; N, 21.34. Found: C, 33.81; H, 4.45; N, 21.19. IR (cm^{-1}, KBr disk): $\nu_{C\equiv N}$ 2194 (m), 2180 (m), 2170 (m), 2144 (w).

Preparation of $\{[Mn_3(bipy)_2(DMF)_8][W(CN)_8]_2\}_\infty$ (2). A solution of $MnCl_2\cdot 4H_2O$ (0.297 g, 1.5 mmol) and 2,2′-bipy (0.468 g, 3.0 mmol) in CH_3OH (30 mL) was added to a solution of $(n\text{-}Bu_4N)_3[W(CN)_8]$ (1.118 g, 1.0 mmol) in CH_3OH (20 mL) with stirring to give a pale yellow precipitate immediately, which was filtered and washed with methanol. Then the precipitate was collected and dissolved in DMF. Brown block crystals were obtained by slow diffusion of diethyl ether into the resulting DMF solution for several days (yield 92%). Anal. Calcd for $C_{60}H_{72}N_{28}O_8Mn_3W_2$: C, 39.04; H, 3.93; N, 21.24; Mn, 8.93. Found: C, 38.96; H, 4.01; N, 21.62; Mn, 9.23. IR (cm^{-1}, KBr disk): $\nu_{C\equiv N}$ 2178 (m), 2158 (m).

Crystal Structure Determination. Single-crystal X-ray data for $\{[Co_3(DMF)_{12}][W(CN)_8]_2\}_\infty$ (**1**) were collected on a Bruker Apex SMART CCD system equipped with monochromated Mo Kα radiation (λ = 0.710 73 Å) at room temperature. The data integration and empirical absorption corrections were carried out by SAINT[12] and SADABS[13] programs, respectively. The structure was solved by direct methods and refined on F^2 using the SHELXTL[14] suite of programs. All non-hydrogen atoms were refined anisotropically by full-matrix least squares. Hydrogen atoms were generated geometrically. For complex **2**, intensity data were collected on an Enraf-Nonius CAD-4 four-circle diffractometer by ω-scan techniques using graphite-monochromated Mo Kα radiation (λ = 0.710 73 Å) at room temperature. Corrections for Lorentz and polarization effects and for absorption (ψ scan) were applied. The structure was solved by direct methods and refined on F^2 using the SHELXTL suite of programs. Except for the disordered carbon and nitrogen atoms of the coordinated DMF molecules (N11, N13, N14, C19, C20, C21, C22, C23, C24, C26, C27, C29, and C30), the majority of the non-H atoms were refined anisotropically. The maximum and minimum residual densities are 2.877 and −2.401 e $Å^{-3}$, respectively, which are within 1.0 Å from W1. The crystallographic data for the two compounds are summarized in Table 1.

Results and Discussion

Synthesis. For complex **1**, we initially hoped to prepare a Co_9W_6 cluster as a single-molecule magnet (SMM) with large anisotropy using the bare metal ion Co^{2+} and $[W(CN)_8]^{3-}$, as for the reported $M_9M'_6$ clusters ($M = Mn^{2+}$, Ni^{2+}; $M' =$ Mo, W).[6a−c] However, it is unexpected that a one-dimensional coordination polymer is obtained and exhibits a structural feature similar to that of complex **2**. For complex **2**, in the reaction recipe, the Mn^{2+} and bipy ratio is 1:2, but in the complex, only 1 bipy to 1.5 Mn^{2+} was found. We

(5) Rombaut, G.; Verelst, M.; Golhen, S.; Ouahab, L.; Mathonière, C.; Kahn O. *Inorg. Chem.* **2001**, *40*, 1151.

(6) (a) Larionova, J.; Gross, M.; Pilkington, M.; Andres, H.; Stoeckli-Evans, H.; Güdel, H. U.; Decurtins, S. *Angew. Chem., Int. Ed.* **2000**, *39*, 1605. (b) Zhong, Z. J.; Seino, H.; Mizobe, Y.; Hidai, M.; Fujishima, A.; Ohkoshi, S.; Hashimoto, K. *J. Am. Chem. Soc.* **2000**, *122*, 2952. (c) Bonadio, F.; Gross, M.; Stoeckli-Evans, H.; Decurtins, S. *Inorg. Chem.* **2002**, *41*, 5891. (d) Podgajny, R.; Desplanches, C.; Sieklucka, B.; Sessoli, R.; Villar, V.; Paulsen, C.; Wernsdorfer, W.; Dromzée, Y.; Verdaguer, M. *Inorg. Chem.* **2002**, *41*, 1323.

(7) (a) Rombaut, G.; Golhen, S.; Ouahab, L.; Mathonière, C.; Kahn, O. *J. Chem. Soc., Dalton Trans.* **2000**, 3609. (b) Li, D.-f.; Gao, S.; Zheng, L.-m.; Tang, W.-x. *J. Chem. Soc., Dalton Trans.* **2002**, 2805.

(8) Podgajny, R.; Korzeniak, T.; Balanda, M.; Wasiutynski, T.; Errington, W.; Kemp, T. J.; Alcock, N. W.; Sieklucka, B. *Chem. Commun.* **2002**, 1138. Li, D.-f.; Zheng, L.-m.; Wang, X.-y.; Huang, J.; Gao, S.; Tang, W.-x. *Chem. Mater.* **2003**, *15*, 2094.

(9) (a) Zhong, Z. J.; Seino, H.; Mizobe, Y.; Hidai, M.; Verdaguer, M.; Ohkoshi, S.; Hashimoto, K. *Inorg. Chem.* **2000**, *39*, 5095. (b) Song, Y.; Ohkoshi, S.; Arimoto, Y.; Seino, H.; Mizobe, Y.; Hashimoto, K. *Inorg. Chem.* **2003**, *42*, 1848. (c) Sra, A. K.; Rombaut, G.; Lahitete, F.; Golhen, S.; Ouahab, L.; Mathonière, C.; Yakhmi, J. V.; Kahn, O. *New J. Chem.* **2000**, *24*, 871. (d) Li, D.-F.; Gao, S.; Zheng, L.-M.; Sun, W.-Y.; Okamura, T.-a.; Ueyama, N.; Tang, W.-X. *New J. Chem.* **2002**, *26*, 485.

(10) Clérac, R.; Miyasaka, H.; Yamashita, M.; Coulon, C. *J. Am. Chem. Soc.* **2002**, *124*, 12837.

(11) Baadsgaard, H.; Treadwell, W. D. *Helv. Chim. Acta* **1955**, *38*, 1669.

(12) SAINT Data Integration Software; Bruker AXS. Inc., Madison, WI, 1997.

(13) Sheldrick, G. M. SADABS Empirical Absorption Correction Program; University of Göttingen, Göttingen, Germany, 1996.

(14) Sheldrick, G. M. SHELXTL Program for Crystal Structure Determinations; Siemens Industrial Automation, Inc.: Madison, WI, 1997.

Table 1. Crystal Data and Structure Refinement Details for $\{[Co_3(DMF)_{12}][W(CN)_8]_2\}_\infty$ (**1**) and $\{[Mn_3(bipy)_2(DMF)_8][W(CN)_8]_2\}_\infty$ (**2**)

	1	**2**
formula	$C_{52}H_{84}N_{28}O_{12}Co_3W_2$	$C_{60}H_{72}N_{28}O_8Mn_3W_2$
M_w	1837.96	1845.98
cryst syst	triclinic	triclinic
space group	$P\bar{1}$	$P\bar{1}$
a/Å	11.690(3)	10.672(2)
b/Å	12.703(3)	13.024(3)
c/Å	13.712(3)	16.000(3)
α/deg	86.889(4)	78.32(3)
β/deg	73.256(4)	75.69(3)
γ/deg	77.033(4)	66.63(3)
V/Å^3	1900.0(8)	1964.4(7)
Z	1	1
ρ_{calcd}/g cm^{-3}	1.606	1.560
μ(Mo Kα)/mm^{-1}	3.727	3.452
no. of rflns collcd	10 892	7270
no. of indep rflns	7940 (R_{int} = 0.0238)	6872 (R_{int} = 0.0654)
GOF on F^2	1.021	1.014
R indices ($I > 2\sigma(I)$)[a]	R1 = 0.0327, wR2 = 0.0644	R1 = 0.0573, wR2 = 0.1398
R indices (all data)	R1 = 0.0388, wR2 = 0.0655	R1 = 0.0998, wR2 = 0.1691

[a] $R1 = \sum||F_o| - |F_c|/\sum|F_o|$; $wR2 = [\sum w(|F_o|^2 - |F_c|^2)|/\sum|w(F_o)^2]^{1/2}$.

have also tried to use $[Mn(bipy)_2(H_2O)](ClO_4)_2$ as the starting material, and the same crystals were obtained. This implies that the bipy ligands coordinated to Mn^{2+} were replaced by cyano groups and/or DMF molecules in the spontaneous self-assembly process of **2**. A similar example has been shown by Dunbar et al. for a Mn_3Fe_2 2-D ferrimagnet.[15]

Description of Structures. Selected bond distances and angles for complexes **1** and **2** are listed in Tables 2 and 3, respectively. The molecular structures of complexes **1** and **2** are shown in Figure 1 and Figure S1 in the Supporting Information.

(a) $\{[Co_3(DMF)_{12}][W(CN)_8]_2\}_\infty$ (1). X-ray crystallographic studies revealed that complex **1** is a neutral, one-dimensional infinite chainlike polymer. The asymmetric unit of the structure consists of one $W^V(CN)_8^{3-}$ moiety connected to two different types of Co^{II} centers by cyanide bridges. The W1 atom is coordinated by eight CN groups, with W−C distances ranging from 2.140(5) to 2.175(4) Å in a distorted bicapped trigonal prism. The two Co atoms are all in a slightly distorted octahedral geometry. The equatorial sites of Co1 are occupied by two oxygen atoms and two nitrogen atoms (O1, O3, N5, and N6^i; $i = -x + 1, -y + 2, -z + 1$), and the apical positions are occupied by two oxygen atoms (O2, O4) from DMF molecules. The other Co atom (Co2), localized at the special equivalent positions (1, $^1/_2$, 0), is coordinated with four oxygen atoms (O5, O6, O5^{ii}, and O5^{ii}) from four DMF molecules occupying the equatorial sites and two nitrogen atoms (N2, N2^{ii}) from two adjacent $W(CN)_8$ units at the axial positions ($ii = -x + 2, -y + 1, -z$). Each $W^V(CN)_8$ group connects three Co atoms (Co1, Co1^i, and Co1^{ii}) via three cyano bridges (C5−N5, C6−N6, and C2−N2) with the Co−N_{CN} distance ranging from 2.096(3) to 2.131(3) Å. W1, Co1, W1^i, and Co1^i were joined by four cyano bridges (C5−N5, C6^i−N6^i, C5^i−N5^i, and C6−N6) to form a 4-metal 12-atom rhombic cycle, $Co_2W_2(CN)_4$, while Co2 links the cycles in a trans mode through W1−C2−N2−Co2−N2^{ii}−C2^i−W1^{ii} linkages to form a 1-D infinite chain, running along one of the diagonal directions of the b and c axes (Figures 1a and 2). This type of 1-D chain has been defined as a 3,2-chain by Černák et al.,[16] which has been found in complexes $\{(DMF)_{10}Ln_2[Ni-$

Table 2. Selected Bond Distances (Å) and Angles (deg) for $\{[Co_3(DMF)_{12}][W(CN)_8]_2\}_\infty$ (**1**)[a]

Bond Distances (Å)			
Co(1)−O(1)	2.111(3)	Co(1)−O(2)	2.083(3)
Co(1)−O(3)	2.097(3)	Co(1)−O(4)	2.068(3)
Co(1)−N(5)	2.131(3)	Co(1)−N(6)^i	2.109(3)
Co(2)−O(5)	2.070(4)	Co(2)−O(6)	2.084(3)
Co(2)−N(2)	2.096(3)	W(1)−C(1)	2.165(4)
W(1)−C(2)	2.164(4)	W(1)−C(3)	2.140(5)
W(1)−C(4)	2.143(5)	W(1)−C(5)	2.162(4)
W(1)−C(6)	2.175(4)	W(1)−C(7)	2.148(5)
W(1)−C(8)	2.148(4)	C(2)−N(2)	1.139(5)
C(5)−N(5)	1.143(5)	C(6)−N(6)	1.139(4)
Bond Angles (deg)			
O(1)−Co(1)−N(5)	85.85(12)	O(2)−Co(1)−O(1)	88.12(12)
O(2)−Co(1)−O(3)	90.63(13)	O(2)−Co(1)−N(5)	89.50(13)
O(2)−Co(1)−N(6)^i	88.52(12)	O(3)−Co(1)−N(6)^i	88.35(12)
O(3)−Co(1)−O(1)	92.03(12)	O(3)−Co(1)−N(5)	177.87(13)
O(4)−Co(1)−O(1)	88.04(12)	O(4)−Co(1)−O(2)	176.16(11)
O(4)−Co(1)−O(3)	89.35(12)	N(6)^i−Co(1)−N(5)	93.78(13)
O(4)−Co(1)−N(5)	90.38(12)	O(5)−Co(2)−N(2)	91.51(14)
O(5)−Co(2)−O(6)	91.97(14)	O(6)−Co(2)−N(2)	93.04(13)
C(2)−N(2)-Co(2)	167.7(4)	C(5)−N(5)-Co(1)	159.9(3)
C(6)−N(6)-Co(1)^i	158.2(3)	C(2)−W(1)-C(6)	130.41(15)
C(5)−W(1)-C(2)	137.54(15)	C(5)−W(1)-C(6)	72.08(14)
N(1)−C(1)-W(1)	178.1(4)	N(2)−C(2)-W(1)	178.0(4)
N(3)−C(3)-W(1)	178.5(4)	N(4)−C(4)-W(1)	177.0(5)
N(5)−C(5)-W(1)	176.1(4)	N(6)−C(6)-W(1)	176.8(3)
N(7)−C(7)-W(1)	178.6(5)	N(8)−C(8)-W(1)	177.1(4)

[a] Symmetry transformation used to generate equivalent atoms: (i) $-x + 1, -y + 2, -z + 1$.

Table 3. Selected Bond Distances (Å) and Angles (deg) for $\{[Mn_3(bipy)_2(DMF)_8][W(CN)_8]_2\}_\infty$ (**2**)[a]

Bond Distances (Å)			
Mn(1)−O(1)	2.206(9)	Mn(1)−O(2)	2.109(9)
Mn(1)−N(1)	2.215(10)	Mn(1)−N(4)^{iii}	2.180(10)
Mn(1)−N(9)	2.262(10)	Mn(1)−N(10)	2.233(9)
Mn(2)−O(3)	2.156(9)	Mn(2)−O(4)	2.159(8)
Mn(2)−N(6)	2.254(9)	N(1)−C(1)	1.128(14)
N(4)−C(4)	1.154(15)	N(6)−C(6)	1.122(14)
W(1)−C(1)	2.169(11)	W(1)−C(5)	2.145(11)
W(1)−C(2)	2.130(11)	W(1)−C(6)	2.188(11)
W(1)−C(3)	2.151(11)	W(1)−C(7)	2.129(10)
W(1)−C(4)	2.157(12)	W(1)−C(8)	2.139(12)
Bond Angles (deg)			
C(4)−W(1)-C(1)	72.8(4)	C(4)−W(1)-C(6)	136.5(4)
C(1)−W(1)-C(6)	124.4(4)	O(2)−Mn(1)-O(1)	178.3(4)
N(4)^{iii}−Mn(1)−O(1)	89.5(4)	N(4)^{iii}−Mn(1)−N(1)	100.9(4)
O(1)−Mn(1)-N(1)	89.9(4)	N(10)−Mn(1)-N(9)	73.4(4)
O(3)−Mn(2)-O(4)	91.1(4)	O(3)−Mn(2)-N(6)	89.9(4)
O(4)−Mn(2)-N(6)	91.1(3)	C(4)−N(4)-Mn(1)^{iii}	171.6(10)
C(1)−N(1)-Mn(1)	175.4(10)	C(6)−N(6)-Mn(2)	156.0(9)
N(1)−C(1)-W(1)	179.4(11)	N(2)−C(2)-W(1)	177.8(13)
N(3)−C(3)-W(1)	176.8(10)	N(4)−C(4)-W(1)	177.9(11)
N(5)−C(5)-W(1)	178.6(13)	N(6)−C(6)-W(1)	175.9(10)
N(7)−C(7)-W(1)	178.4(13)	N(8)−C(8)-W(1)	178.6(11)

[a] Symmetry transformation used to generate equivalent atoms: (iii) $-x + 2, -y + 1, -z + 1$.

(15) Smith, J. A.; Galán-Mascarós, J.-R.; Clérac, R.; Dunbar, K. R. *Chem. Commun.* **2000**, 1077.

(16) Čěrnák, J.; Orendáč, M.; Potočňák, I.; Chomič, J.; Orendáčová, A.; Skoršepa, J.; Feher, A. *Coord. Chem. Rev.* **2002**, *224*, 51.

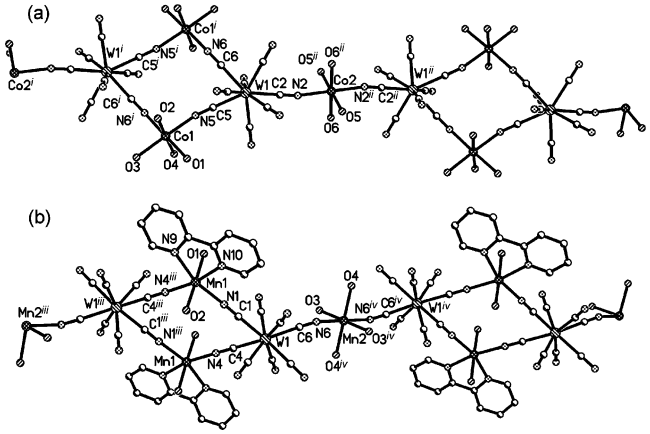

Figure 1. Molecular structures for (a) complex **1** and (b) complex **2**, showing a fragment of the one-dimensional infinite structure with the atom-labeling scheme. The hydrogen atoms and the C and N atoms of the coordinated DMF molecules are omitted for clarity. Symmetry operations: (*i*) $-x+1, -y+2, -z+1$; (*ii*) $-x+2, -y+1, -z$; (*iii*) $-x+2, -y+1; -z+1$; (*iv*) $-x+2, -y, -z+2$.

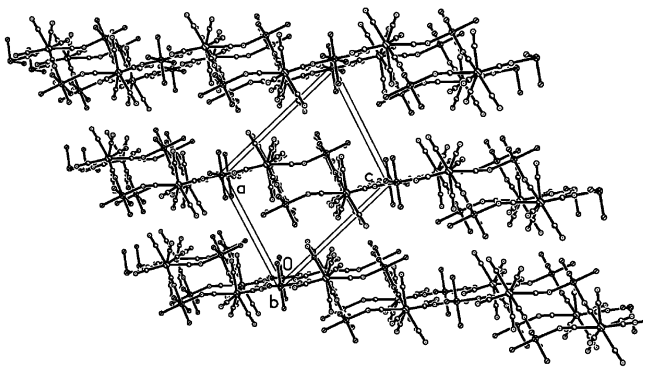

Figure 2. Packing diagram of complex **1** in the *ac* plane. The hydrogen atoms and the C and N atoms of the coordinated DMF molecules are omitted for clarity.

$(CN)_4]_3\}_\infty$ (Ln = Sm, Yb, Er).[17] In complex **1**, the shortest metal···metal intrachain distances for W1···Co1, W1···Co2, Co1···Co2, W1···W1^{i}, and Co1···Co1^{i} are 5.335(1), 5.363(1), 10.252(2), 8.443(1), and 6.491(2) Å, respectively. The adjacent chains are separated well by the coordinated DMF molecules, with a distance of 11.690(3) Å along the *a* axis (Figure 2). No pronounced hydrogen-bonding interaction, except the van der Waals force between the chains, can be found.

(b) $\{[Mn_3(bipy)_2(DMF)_8][W(CN)_8]_2\}_\infty$ (2). The structure of **2** reveals that the complex is also a neutral, one-dimensional infinite polymer, similar to complex **1**. The asymmetric unit of the structure consists of one $W^V(CN)_8^{3-}$ moiety connected to two different types of Mn^{II} centers by cyanide bridges. The W1 atom is coordinated by eight CN groups with W−C distances ranging from 2.129(10) to 2.188(11) Å in a distorted bicapped trigonal prism. The two Mn atoms are all in a slightly distorted octahedral geometry (Figure 1b). For Mn1, the equatorial sites are occupied by four nitrogen atoms, N1, N4^{iii}, N9, and N10, with an average Mn−N distance of 2.22 Å (*iii* = $-x+2, -y+1, -z+1$),

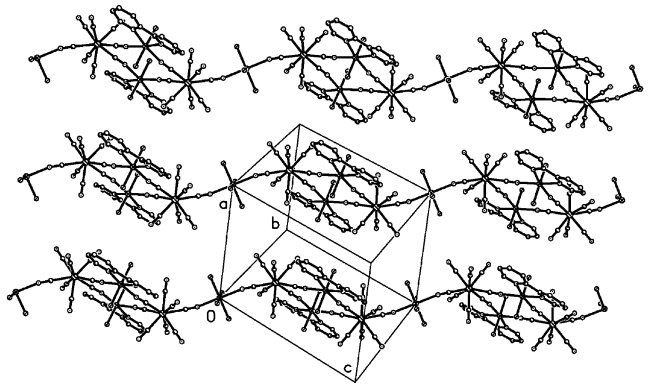

Figure 3. Packing diagram of complex **2**. The hydrogen atoms and the C and N atoms of the coordinated DMF molecules are omitted for clarity.

while the apical positions are occupied by two oxygen atoms (O1, O2) from two DMF molecules. The other Mn atom (Mn2), localized at the special equivalent positions (1, 0, 1), are coordinated with four oxygen atoms (O3, O4, O3^{iv}, and O4^{iv}) from four DMF molecules occupying the equatorial sites and two nitrogen atoms (N6, N6^{iii}) from two adjacent $W(CN)_8$ units at the axial positions (*iv* = $-x+2, -y, -z+2$). Each $W^V(CN)_8$ group connects three Mn atoms (Mn1, Mn1^{iii}, and Mn2) via three cyano bridges (C1−N1, C4−N4, and C6−N6), with the Mn−N_{CN} distance ranging from 2.180(10) to 2.254(9) Å. Similar to the case for **1**, W1, Mn1, W1^{iii}, and Mn1^{iii} were linked by four cyano bridges (C1−N1, C4^{iii}−N4^{iii}, C1^{iii}−N1^{iii}, and C4−N4) to form a 4-metal 12-atom rhombic cycle, $Mn_2W_2(CN)_4$, while Mn2 links the rhombic cycles in a trans mode through W1−C6−N6−Mn2−N6^{iv}−C6^{iv}−W1^{iv} linkages to form a 1-D 3,2-chain, running along one of the diagonal directions of the *b* and *c* axes (Figure 1b). The shortest metal···metal intrachain distances for W1···Mn1, W1···Mn2, Mn1···Mn2, W1···W1^{iii}, and Mn1···Mn1^{iii} are 5.508(2), 5.417(2), 10.028(3), 8.714(3), and 6.693(4) Å, respectively. The nearest interchain distances are separated by the coordinated DMF and bipy molecules with a distance of 10.672(2) Å along the *a* axis (Figure 3). Unlike complex **1**, however, in complex **2** there is a weak interaction between the one-dimensional chains via $\pi-\pi$ stacking existing between the adjacent interchain aromatic rings of 2,2′-bipyridine, at a face-face distance of 3.95 Å. The reason for the smaller interchain separation in **2** can be attributed to the bipy ligands replacing two DMF molecules in **1**.

Magnetic Studies. (a) $\{[Co_3(DMF)_{12}][W(CN)_8]_2\}_\infty$ (1). The temperature dependence of the magnetic susceptibility, χ_M, can be fit by the Curie−Weiss law, with $g^W = 2.0$ ($S = {}^1/_2$), $g^{Co} = 2.84$ ($S = {}^3/_2$), and $\Theta = +14.44$ K ($T > 25$ K), indicative of ferromagnetic coupling between the W(V) and Co(II) metal centers (Figure 4). At room temperature, $\chi_M T$ is 12.68 cm^3 mol^{-1} K (10.07 μ_B) per Co_3W_2, close to the expected spin-only value (12.09 cm^3 mol^{-1} K, 9.83 μ_B per Co_3W_2) for three Co(II) ($S = {}^3/_2$, $g = 2.84$) and two W(V) ($S = {}^1/_2$, $g = 2.0$) centers. As the temperature is lowered, the $\chi_M T$ value monotonically increases and then increases abruptly up to a maximum value of 46.78 cm^3 mol^{-1} K (23.90 μ_B) at 14 K, followed by a drop to 12.75 cm^3 mol^{-1}

(17) Knoeppel, D. W.; Liu, J.; Meyers, E. A.; Shore, S. G. *Inorg. Chem.* **1998**, *37*, 4828. Knoeppel, D. W.; Shore, S. G. *Inorg. Chem.* **1996**, *35*, 1747.

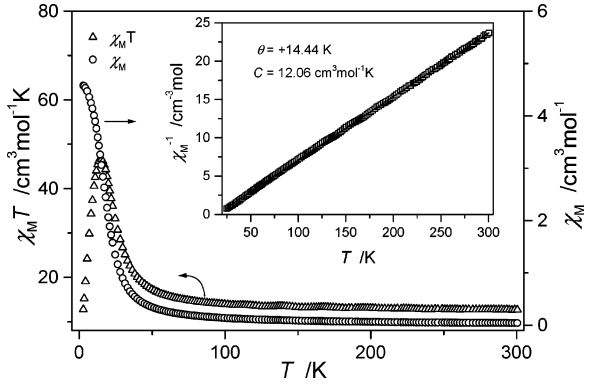

Figure 4. Plots of χ_M (○) and $\chi_M T$ (△) vs T in the range of 2−300 K at 1 kOe for complex **1** per Co_3W_2 unit. Inset: plot of χ_M^{-1} vs T in the range of 25−300 K (the solid line is the best fit based on the Curie−Weiss law).

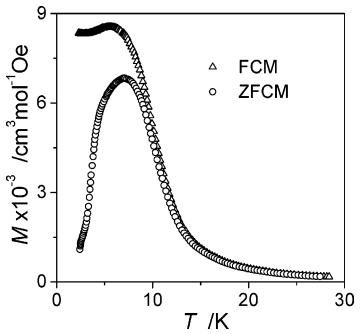

Figure 5. Plots of field-cooled magnetization (FCM, △) and zero-field-cooled magnetization (ZFCM, ○) vs temperature measured at 100 Oe for complex **1**.

K (10.10 μ_B) at 2.8 K. The abrupt increase in $\chi_M T$ suggests the onset of magnetic ordering, and the decrease of $\chi_M T$ below 14 K results from a saturation of the χ_M value and/or the zero-field splitting effect.

The FCM and ZFCM data for complex **1** diverge below ca. 10 K, the FCM continuing to increase and approach a plateau value, while the ZFCM data show a peak at ca. 7 K (Figure 5). This may imply the presence of long-range magnetic ordering in complex **1**. To probe the nature of long-range ordering in **1**, the temperature dependence of linear ac molar magnetic susceptibilities was performed at zero field below 9 K (Figure 6). It can be seen that the susceptibility data are evidently frequency dependent. For all frequencies used, the in-phase component of the ac susceptibility, χ_M', shows a rounded maximum in the ranges 6−8 K. This is always accompanied by a maximum in the out-of-phase component, χ''_M, at somewhat lower temperature with decreasing frequencies. The peak temperature of χ_M' increases and the peak height decreases with increasing frequency, implying a slow relaxation process. The shift in temperature of maxima in χ'_M and χ''_M with the frequency are reminiscent of single-molecule magnet (SMM), spin-glass, superparamagnetic, or the recently reported single-chain magnet (SCM) behavior. We tried to obtain the relaxation time (τ) from the Arrhénius law:[10]

$$\tau(T) = \tau_0 \exp(\Delta/(k_B T))$$

The best-fit parameters are $\tau_0 = 2.3 \times 10^{-15}$ s and $\Delta/k_B = 170(3)$ K (see Figure S3 in the Supporting Information). The

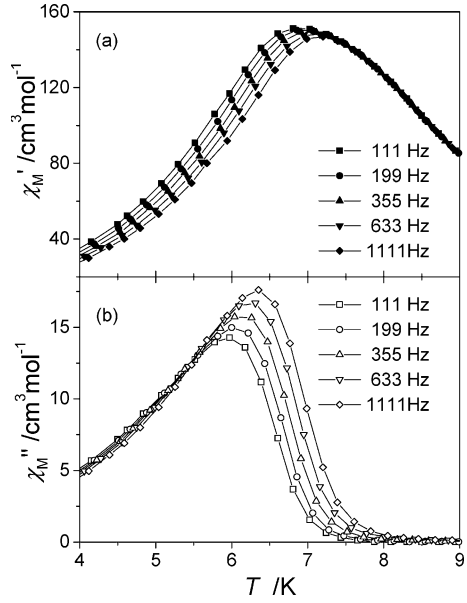

Figure 6. Temperature and frequency dependence of the (a) real (χ_M') and (b) imaginary (χ_M'') parts of the ac susceptibility ($H_{dc} = 0$ Oe, $H_{ac} = 2$ Oe) for complex **1**.

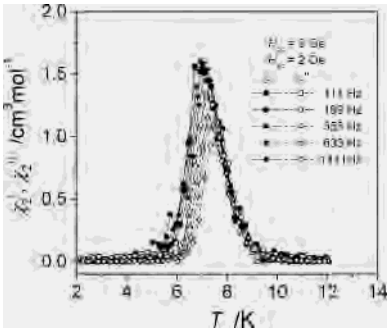

Figure 7. Nonlinear susceptibilities $|\chi_2|$ of complex **1** measured at 2f in $H_{ac} = 2$ Oe (zero applied dc field) with frequency 111−1111 Hz.

value of τ_0 is rather fast compared with that of SMM or SCM,[10] which preclude the possibility of single-chain magnet behavior for complex **1**. A quantitative measure of the frequency shift is obtained from $\phi = \Delta T_p/[T_p \Delta(\log f)]) = 0.08$, which places the compound **1** in the range of a spin glass and excludes a superparamagnet.[18]

Even harmonics can be observed only if a system exhibits a spontaneous magnetization, due to the lack of inversion symmetry with respect to the applied field. Only odd harmonics are expected for a spin glass, while for ferromagnets both even and odd harmonics should be present.[19−22] The second harmonics (2f responses) for complex **1** have sharp peaks (Figure 7), which indicates that a spontaneous moment is formed at that transition (ca. 7.3 K) while the frequency dependence of both components of the nonlinear

(18) Mydosh, J. A. *Spin Glasses: An Experimental Introduction*; Taylor and Francis: London, 1993.
(19) Gîrţu, M. A.; Wynn, C. M.; Fujita, W.; Awaga, K.; Epstein, A. J. *Phys. Rev. B* **1998**, *57*, 58.
(20) Gîrţu, M. A.; Wynn, C. M.; Fujita, W.; Awaga, K.; Epstein, A. J. *J. Appl. Phys.* **1998**, *83*, 7378.
(21) Androulakis, J.; Katsarakis, N.; Giapintzakis, J. *J. Appl. Phys.* **2002**, *91*, 9952.
(22) Bajpai, A.; Banerjee, A. *Phys. Rev. B* **2000**, *62*, 8996.

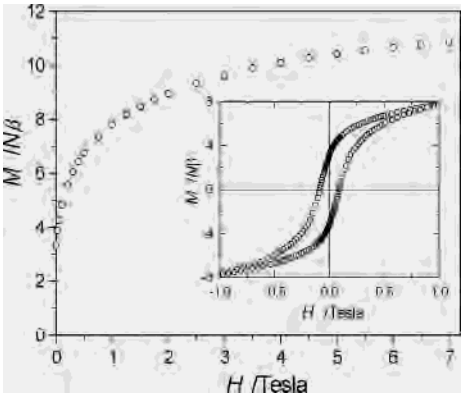

Figure 8. Field dependence of the magnetization at 1.8 K for complex **1** per Co_3W_2 unit. Insert: hysteresis loop ($M/N\beta$ vs H) at 1.8 K.

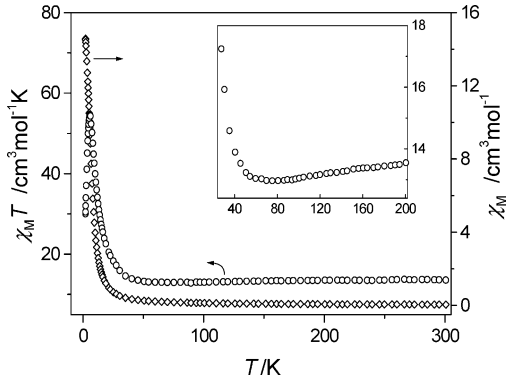

Figure 9. Plots of χ_M (◇) and $\chi_M T$ (○) vs T in the range of 2−300 K for complex **2** per Mn_3W_2 unit. Inset: expanded view of the minimum region of $\chi_M T$.

susceptibility suggests slow relaxation processes and glassiness. Nonzero values of χ_3' (Figure S4 in the Supporting Information) could be attributed to the irreversible domain-wall motion.[23] Thus, complex **1** should be a long-range-ordering ferromagnet, but with some glassy behavior or possible related blocking of the domain wall.[21,24]

The field dependence of the magnetization (0−7 T) measured at 1.8 K shows a rapid increase from zero field (Figure 8). At 7 T, the magnetization reaches 10.85 $N\beta$, close to the saturation value 11.0 $N\beta$ for three Co(II) and two W(V) atoms. A hysteresis loop at 1.8 K was observed with a rather large coercive field of ca. 907 Oe and a remnant magnetization of ca. 3.39 $N\beta$.

(b) $\{[Mn_3(bipy)_2(DMF)_8][W(CN)_8]_2\}_\infty$ (2). The dc variable-temperature (2−300 K) magnetic susceptibility of the complex has been measured on a crystalline sample in a field of 1 kOe. Plots of $\chi_M T$ vs T and χ_M vs T are shown in Figure 9, where χ_M is the magnetic susceptibility per Mn_3W_2 unit. The $\chi_M T$ value at room temperature is ca. 13.56 cm^3 K mol^{-1} (10.41 μ_B per Mn_3W_2), which is slightly smaller than the spin-only value (13.875 cm^3 K mol^{-1}, 10.50 μ_B) for three high-spin Mn(II) ($S = {}^5/_2$) and two W(V) ($S = {}^1/_2$) centers with $g = 2.0$. As T is lowered, $\chi_M T$ decreases smoothly and reaches a minimum value of 12.96 cm^3 K mol^{-1} (10.18 μ_B)

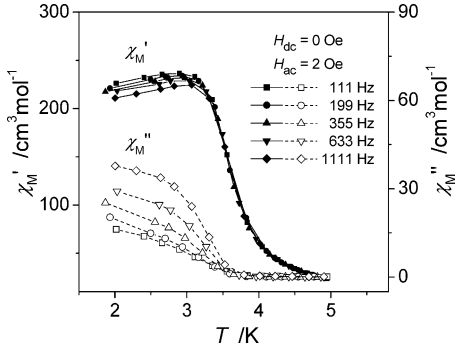

Figure 10. Temperature dependence of zero-field ac susceptibility for complex **2**, measured at 2 Oe ac field with frequency 111−1111 Hz.

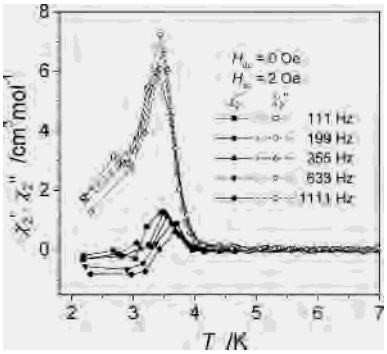

Figure 11. Nonlinear susceptibilities χ_2 of complex **2** measured at 2f in $H_{ac} = 2$ Oe (zero applied dc field) with frequency 111−1111 Hz.

around 75 K. Upon further cooling, the value of $\chi_M T$ increases rapidly, reaching a sharp maximum value of 54.60 cm^3 K mol^{-1} (20.90 μ_B) around 5.6 K. The minimum in the $\chi_M T$ vs. T curve indicates a ferrimagnetic behavior with a $Mn^{II}-W^V$ intrachain antiferromagnetic interaction, and the maximum value in the curve, much larger than the above-mentioned spin-only value, suggests the occurrence of long-range magnetic ordering. Below 5.6 K, the value of $\chi_M T$ decreases abruptly, while the χ_M value increases slowly at low temperature. This indicates that the decrease of $\chi_M T$ below 5.6 K should be attributed to the saturation of the χ_M value. The magnetic susceptibility above 75 K obeys the Curie−Weiss law ($1/\chi_M = (T - \Theta)/C$) with a negative Weiss constant, Θ, of −3.64 K (Figure S5, Supporting Information), which also indicates an intramolecular antiferromagnetic coupling between the adjacent Mn(II) and W(V) ions through the cyano bridges. The Curie constant, C, is equal to 13.75 cm^3 K mol^{-1}, close to the expected value of 13.875 cm^3 K mol^{-1} with $g = 2.0$.

Both the zero-field-cooled magnetization (ZFCM) and field-cooled magnetization (FCM) curves measured in a low field of 100 Oe show a rapid increase in M at ca. 3.5 K, implying the occurrence of spontaneous magnetization at this point. Figure 10 shows the linear ac magnetic susceptibility with different frequencies. Similar to compound **1**, the susceptibility data are also frequency dependent, indicative of spin-glass behavior for compound **2**. The nonlinear ac susceptibility measurement for **2** has also been performed to confirm the spontaneous ferromagnetic ordering (Figure 11). The second harmonics (2f responses) for complex **2** exhibit sharp peaks at ca. 3.5 K and are frequency dependent,

(23) Gencer, A.; Ercan, I.; Özçelik, B. *J. Phys.: Condens. Matter*. **1998**, *10*, 191.
(24) Evangelisti, M.; Bartolomé, J.; de Jongh, L. J.; Filoti, G. *Phys. Rev. B* **2002**, *66*, 144410.

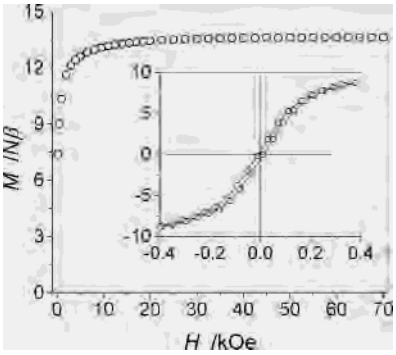

Figure 12. Field dependence of the magnetization at 1.8 K for complex **2** per Mn_3W_2 unit. Insert: hysteresis loop ($M/N\beta$ vs H) at 1.8 K.

which demonstrates that complex **2** is a ferrimagnet with glassy behavior.

The field dependence of the magnetization (0−7 T) measured at 1.8 K shows a rapid increase with applied field and rapid increase of the magnetization, as a magnet, reaching 13.07 $N\beta$ per Mn_3W_2 at 907 Oe, very close to the expected $S_T = {}^{13}/_2$ value of 13 $N\beta$ for a ferrimagnetic $Mn^{II}{}_3W^{V}{}_2$ ($^5/_2 \times 3 - {}^1/_2 \times 2 = {}^{13}/_2$) system, assuming $g = 2.0$ (Figure 12). A hysteresis loop at 1.8 K was observed with a small coercive field less than 10 Oe, indicating that compound **2** is typical of a soft magnet.

The compound $Mn_3{}^{II}W_2{}^{V}$ (**2**) is isomorphous with its Mo^V analogue,[7b] $\{[Mn_3(bipy)_2(DMF)_8][Mo(CN)_8]_2\}_\infty$ (**3**), and their magnetic properties are also similar. Complex **3** exhibits long-range magnetic ordering at ca. 2.8 K and shows weak frequency dependence (Figure S7, Supporting Information). Its phase transition value is smaller than that of complex **2**. This should be due to the fact that the 5d orbitals of W^V atom are more diffuse than the 4d orbitals of the Mo^V atom, and thus, a stronger magnetic interaction for W^V-Mn^{II} is expected. For the three 1-D compounds, similar magnetic properties should be attributed to their similar 3,2-chain structures.

For compounds **1** and **2**, the coupling nature of $Co^{II}-W^V$ in **1** is found to be ferromagnetic but the magnetic interaction $Mn^{II}-W^V$ in compound **2** is antiferromagnetic. Recently, there were a few reported examples of antiferromagnetic coupling for a cyano-bridged $Mn^{II}-W^V$ system,[6b,9a,b] and the origin of antiferromagnetism has been analyzed within the Anderson super-exchange theory.[9b,25] The ferromagnetic coupling $Co^{II}-W^V$ system has not been reported until now; however, the origin of ferromagnetism might be interpreted by Chibotau's analysis as an analogue of $[Nb^{IV}\{(\mu\text{-}CN)_4\text{-}Co^{II}(H_2O)_2\}]$.[25]

Reports of one-dimensional cyano-bridged polymers exhibiting long-range ferromagnetic ordering have been rare to date.[26] In 1996, Matsumoto et al. reported a one-dimensional ferromagnet, $[NEt_4]_2[Mn(acacen)][Fe(CN)_6]$ (acacen = *N*,*N*′-ethylenebis(acetylacetonylideneaminato)), in which an intrachain ferromagnetic coupling exists between the high-spin Mn(III) and the low-spin Fe(III) via the bridging cyanide anions, while the chains weakly couple to each other ferromagnetically, thus giving a ferromagnet with T_C below 2.5 K.[27] Okawa's group[26,28] has investigated the magneto-structural correlation of a series of one-dimensional cyanide-bridged bimetallic assemblies over the past few years and has come to the conclusion that the ferromagnetic ordering over the lattice in these compounds will be overcome by the antiferromagnetic interaction between the chains, which is not negligible when the separation between the chains is smaller than 10 Å. In our case, the X-ray structural analyses have shown that the one-dimensional chains are well separated by DMF molecules or bipy ligands, and the nearest interchain separations are larger than 10 Å. Even such a weak interchain interaction, van der Waals forces in **1** and $\pi-\pi$ stacking in **2** and **3**, should have a role in the bulk magnetism. The origin of glassy behavior of the compounds may derive from the disorder of the coordinated DMF molecules; further work is underway to understand its nature.

Conclusion

Two new cyano-bridged 3d−5d bimetallic polymers, $\{[Co_3(DMF)_{12}][W(CN)_8]_2\}_\infty$ (**1**) and $\{[Mn_3(bipy)_2(DMF)_8][W(CN)_8]_2\}_\infty$ (**2**), have been obtained and structurally characterized. X-ray crystallography for the two compounds reveals that the two complexes are neutral one-dimensional 3,2-chainlike cyano-bridged bimetallic coordination polymers with 12-atom rhombic $W_2M_2(CN)_4$ (M = Co^{II} (**1**), Mn^{II} (**2**)) units. Magnetic property studies reveal the coexistence of long-range ferromagnetic ordering and glassy behavior in the two compounds. The magnetic phase transition temperatures for complexes **1** and **2** were determined to be around 7.3 and 3.5 K, respectively. Compound **1** exhibits a rather larger coercive field (907 Oe) as compared to that of complex **2** and other reported magnets based on octacyanometalates.

Acknowledgment. We thank the National Natural Science Foundation of China and the National Key Project for Fundamental Research for financial support and Dr. R. Clérac (Centre de Recherche Paul Pascal, CNRS UPR 8641, Pessac, France) for valuable discussions.

Supporting Information Available: Additional figures giving another ORTEP view and magnetic susceptibility plots and X-ray crystallographic files in CIF format for the two compounds. This material is available free of charge via the Internet at http://pubs.acs.org.

IC034539K

(25) Chibotaru, L. F.; Mironov, V. S.; Ceulemans, A. *Angew. Chem., Int. Ed.* **2001**, *40*, 4429 and references therein.
(26) hba, M.; Okawa, H. *Coord. Chem. Rev.* **2000**, *198*, 313 and references therein.
(27) Re, N.; Gallo, E.; Floriani, C.; Miyasaka, H.; Matsumoto, N. *Inorg. Chem.* **1996**, *35*, 6004.
(28) Ohba, M.; Fukita, N.; Okawa, H. *J. Chem. Soc., Dalton Trans.* **1997**, 1733. Ohba, M.; Uauki, N.; Fukita, N.; Okawa, H. *Inorg. Chem.* **1998**, *37*, 3349.